Detection of pith location in chestnut lumber (Mill.) by means of acoustic tomography and longitudinal stress-wave velocity

R. A. Mariño, M. E. Fernández, C. Fernández-Rodríguez, M. Méndez

Draft Manuscript for Review

Detection of pith location using acoustic tomography: an application to longitudinal stress-wave velocity in chestnut lumber (Castanea sativa Mill.)

Journal:	*Holz als Roh- und Werkstoff*
Manuscript ID:	HRW-08-0153.R1
Manuscript Type:	ORIGINALARBEITEN / ORIGINALS
Keywords:	nondestructive evaluation, stress-wave velocity, acoustic tomography, chestnut lumber

Detection of pith location in chestnut lumber (*Castanea sativa* Mill.) by means of acoustic tomography and longitudinal stress-wave velocity

Mariño RA*, Fernández ME, Fernández-Rodríguez C, Méndez M

Department of Agroforestry Engineering. University of Santiago de Compostela. Escuela Politécnica Superior, Campus Universitario s/n, Lugo-27002, Spain.

**Corresponding author: RA Mariño Allegue. Escuela Politécnica Superior, Campus Universitario s/n, Lugo-27002, Spain.*

E-mail: r.allegue@usc.es

Abstract

The objective of this paper was to detect pith location in chestnut lumber by using acoustic tomography techniques. To this end, the velocity gradient was analysed by relating the value of longitudinal stress-wave velocity to the distance from the point where velocity was measured to the pith. A commercial stress-wave timer was used to measure longitudinal stress-wave velocity in 100 x 200 x 400 mm^3 pieces of chestnut lumber (*Castanea sativa* Mill.) obtained from mature trees. The analysed pieces were conditioned to 20% moisture content. Results were classified according to the distance from the point at which velocity was measured to the pith. ANOVA revealed significant differences for mean velocity between the values obtained nearest the pith (at less than 40.0 mm) and the values obtained farthest from the pith. Velocity increased with distance to pith. The coefficient of determination for the linear regression between both variables was R^2 = 0.96. The results of the tests showed a statistically significant relationship between longitudinal velocity and distance to pith. Such results allowed for the estimation of pith location in the area with the lowest velocity values.

Bestimmung der Lage der Markröhre in Kastanienschnittholz (Castanea sativa Mill.) mittels akustischer Tomographie und longitudinaler Stosswellengeschwindigkeit

Zusammenfassung

Ziel dieser Studie war die Bestimmung der Lage der Markröhre in Kastanienschnittholz mittels akustischer Tomographie und Analyse des Geschwindigkeitsgradienten. Dazu wurde der Wert der longitudinalen Stosswellengeschwindigkeit auf den Abstand der Messstelle zur Markröhre bezogen. Ein Stress-Wave-Timer wurde zur Messung der longitudinalen Stosswellengeschwindigkeit an 100 x 200 x 400 mm^3 großen Kastanienholzproben (Castanea sativa Mill.) von adulten Bäumen verwendet. Die analysierten Proben wurden auf eine Holzfeuchte von 20% klimatisiert. Die Ergebnisse wurden nach dem Abstand der Messstelle zur Markröhre ausgewertet. ANOVA ergab signifikante Unterschiede für die mittlere Geschwindigkeit im marknahen Bereich (Abstand kleiner 40 mm) und den markfernen Werten. Die Geschwindigkeit hat sich mit zunehmendem Abstand vom Mark erhöht. Das Bestimmtheitsmaß bei linearer Regression zwischen beiden Variablen betrug R^2 = 0,96. Die Versuchsergebnisse zeigten eine statistisch signifikante Beziehung zwischen der longitudinalen Geschwindigkeit und dem Markabstand. Damit war es möglich, die Lage der Markröhre im Bereich der niedrigsten Geschwindigkeit zu bestimmen

Editorial Office, TU MÃ¼nchen, Holzforschung MÃ¼nchen, Winzererstr. 45, 80797 MÃ¼nchen, Germany

Introduction

Nondestructive evaluation methods comprise impact-induced stress wave techniques. As suggested by Wang et al. (2001a), the impact-induced stress wave method has been extensively studied because of good signal transmission in wood and low cost of equipment. The equipment used includes time of flight tools. A number of authors have studied this type of acoustic tools (Chauhan et al. 2005; Grabianowski et al. 2006).

Evaluation of standing trees is an example of the use of acoustic techniques, which allow for the determination of the presence, size and location of internal decay in standing trees (Nanami et al. 1992; Lawday and Hodges 2000; Divos and Szalai 2003; Rinn 2003, 2004; Wang et al. 2004a). Yet, Deflorio et al. (2008) have suggested that detection of incipient decay at the periphery of tree stems (namely, Douglas fir, beech, oak, and sycamore trees) needs to be improved. As suggested by Ross et al. (1994) for red oak, the use of acoustic techniques prior to kiln-drying allows for separation of infected logs. Such techniques have proved to be effective not only in green wood, but also in the detection of decay in ancient wood (Lee and Oh 1999).

In addition, nondestructive stress-wave techniques can be used to assess how forests can be managed in order to meet desired wood and fibre qualities (Wang et al. 2001b; 2005). Some authors have found a relationship between stress-wave velocity and the mechanical properties of sawn timber. Wagner et al. (2003) reported that intensive stress-wave scanning of Douglas-fir trees could improve the prediction of dynamic modulus of elasticity (MOE) of lumber sawn from the trees.

Editorial Office, TU MÃ¼nchen, Holzforschung MÃ¼nchen, Winzererstr. 45, 80797 MÃ¼nchen, Germany

The application of stress-wave techniques can be useful in sorting logs. Wang et al. (2004b) suggested that the longitudinal stress-wave technique had potential in sorting logs and cants for the production of high MOE products. Ross et al. (2005) found stress wave testing of peeler cores to be a good predictor of static and dynamic modulus of elasticity. Even small-diameter logs could be sorted with reasonable accuracy by using these techniques (Wang et al. 2002). Íñiguez et al. (2007) found a strong correlation between the dynamic modulus obtained by longitudinal vibration frequency and the mechanical properties of large cross-section European black pine members.

Furthermore, stress-wave techniques can be used to relate the characteristics of logs and the characteristics of veneer from logs. Ross et al. (1999) found a strong relationship between log and veneer nondestructive assessments for ponderosa pine, while Rippy et al. (2000) found a strong correlation between Douglas-fir logs and veneer.

However, some characteristics of wood can affect the results of the application of stress-wave techniques. Katz et al. (2008) suggested that modelling the properties of wood is a complex task because of material symmetry changes, and they provided the following examples: lignin (isotropic), hemicelluloses and cellulose (transversely isotropic) and cells and microstructure (orthotropic symmetry). With regard to strength properties, the adverse influence of juvenile wood on such properties should be considered for the effective management of the species (Adamopoulos et al. 2007). According to Chauhan et al. (2007), there is no valid basis for the use of stress-wave velocity to determine growth stress levels in standing trees or in seasoned wood.

Editorial Office, TU MÃ¼nchen, Holzforschung MÃ¼nchen, Winzererstr. 45, 80797 MÃ¼nchen, Germany

Log dimensions may affect stress-wave velocity. Chauhan and Walker (2006) found differences between measurements using two methods for older and large diameter trees. Divos et al. (2005) obtained similar results for board specimens. The results reported by Wang et al. (2004c) indicated that the longitudinal stress-wave velocity technique was sensitive to the size and geometrical imperfections of logs. Marchal and Jacques (1999) evaluated two acoustic methods of MOE determination for young hybrid larch wood, and included specific gravity, ring width and the presence of compression wood in the analysis. Grabianowski et al. (2006) compared acoustic measurements on standing trees, logs and green lumber, and found that external measurements on the log correlated well with measurements for lumber cut adjacent to the bark and modestly with measurements for the corewood. In addition, the authors found that the acoustic velocity in young trees prior to heartwood formation increased from pith to bark.

Moisture content affects the application of stress wave techniques. Wu (1999) reported on the effect of moisture content on wood panels, showing that stress-wave velocity decreased in general with increasing panel moisture content. However, Simpson and Wang (2001) found a strong linear relationship between relative transit time and average moisture content in kiln-dried sugar maple and ponderosa pine boards. Brashaw et al. (2004) found a strong linear relationship between green and dry stress-wave velocity for Southern-pine and Douglas-fir veneers. At a given moisture content level, stress-wave velocity varies with panel type and test directions (Han et al. 2006).

The objective of this paper was to detect pith location using acoustic tomography techniques. The velocity gradient or variation was measured in pieces of chestnut lumber (*Castanea sativa* Mill.) obtained from mature trees. The stress-wave

Editorial Office, TU MÃ¼nchen, Holzforschung MÃ¼nchen, Winzererstr. 45, 80797 MÃ¼nchen, Germany

velocity data obtained using acoustic tomography was related to the distance from the test point to the pith.

Materials and Methods

A total of 432 tests were performed on six chestnut specimens (*Castanea sativa*) with dimensions of 100 x 200 x 400 mm^3 (Figure 1-1). The length of every specimen was parallel to the grain. Because the test moisture content was set at 20%, specimens were previously conditioned to 20% moisture content. All the specimens contained pith and heartwood because all of them had been obtained from a tree with an estimated age of at least 45 years.

Tests were performed using a commercial impact stress-wave device, Arbotom® (copyright © 2005 Frank Rinn, Heidelberg). Arbotom® was initially developed for detecting internal rot, decay and splits on standing trees by using a number of sensors placed around the tree trunk (Rinn 1999). Each sensor was equipped with a vibrometer and electronic regulation for direct real-time analysis of incoming impulses. Because sensors could either emit or receive the signal, reading was taken every time one of the sensors placed around the tree trunk was tapped. In addition to the vibrometer, the sensors contained processing units to digitise and interpret the signals. The sensors were connected in a line with connecting cables. They were attached to the piece of lumber by steel pins via the holding device. The shock bolt was at the front. The impulse waves were induced into the tree via the shock bolts.

The Arbotom-Software was designed to record the data and display them in a matrix, a line or a surface graph. The following data were recorded: sensor

Editorial Office, TU MÃ¼nchen, Holzforschung MÃ¼nchen, Winzererstr. 45, 80797 MÃ¼nchen, Germany

positions, distances, runtimes and velocities, and percent errors. The impulse velocities were calculated from the runtimes and distances between sensors.

The time the stress waves travelled between the sensors was recorded (time-of-flight, TOF) and transferred into velocities. To minimize variations caused by inconsistency in hammer tapping, acoustic measurements were repeated several times for each position of the sensors. The measurements that were too far from the mean value of the previous measurements were rejected.

The test equipment used was composed of 12 sensors, a battery pack, connecting cables between the sensors, a main cable (between battery pack and first sensor) and a personal computer including the Arbomat^{TM} software to record tomography data and to represent data in a table or graph (Rinntech 2005).

Tests were performed on the two end cross-sections of every specimen, which were cut perpendicular to the grain. The dimensions of the cross-sections were 100 x 200 mm^2. Test data were obtained in the longitudinal direction or parallel to the grain. Figure 1-2 shows the cross-sections or sides of the specimens tested. The first step was to establish the position of the sensors.

The two cross-sections of every specimen, named sides A and B, were divided into 20x20 mm^2 squares. Thus, a grid of perpendicular lines was generated. More specifically, four columns and nine rows were generated. One sensor was installed at each point of intersection of two perpendicular lines, such that measurements were collected at different locations in relation to the pith. The distance to the pith centre was measured at every point of intersection. Figure 2 shows the arrangement of the points where sensors were installed.

Editorial Office, TU MÃ¼nchen, Holzforschung MÃ¼nchen, Winzererstr. 45, 80797 MÃ¼nchen, Germany

Specimens were supported at two points near the edges of the specimens, as shown in Figure 3. Four sensors were used (numbered 1, 2, 3 and 4), two of them worked as emitters and two as receivers. As shown in Figure 3, two sensors were placed on Side A (1 and 3) and two on Side B (2 and 4) at opposite positions, such that receivers were paired: 1-2 and 3-4 (the sensors 1 and 3 were placed directly opposite to sensors 2 and 4, respectively). Measurements were taken by acting on Side A sensors, while the stress wave was received by Side B sensors. Similarly, the stress wave emitted by acting on Side B sensors was received by Side A sensors. On each side, sensors were placed in the same row and alternate columns, such that two measurements (M1 and M2) were collected from each sensor. Measurements were collected by tapping Side A sensors first and Side B sensors afterwards. Each sensor was tapped at least ten times during each test. A total of 36 tests were performed per side, such that 36 TOF measurements and 36 measurements of velocity of wave propagation were obtained. Overall, 432 tests were performed with 72 tests per specimen. In addition to the measurements collected during each test, the distance from pith to test point was measured.

Data acquired by using the equipment described above were organized and processed by using SPSS statistical package (Copyright © SPSS Inc., 1989-2006). The statistical analysis of data included ANOVA and post-hoc comparisons between the longitudinal stress-wave velocity obtained at each sensor position and the position of the sensor in relation to the pith. In addition, the correlation between the variables was determined and linear regression analysis was performed.

Editorial Office, TU MÃ¼nchen, Holzforschung MÃ¼nchen, Winzererstr. 45, 80797 MÃ¼nchen, Germany

Results and discussion

Figure 4 shows an example of a tomogram for Specimen 2. The tomogram was obtained using data from ten sensors, five on each cross-section. The lighter shades on the tomogram correspond to higher longitudinal stress-wave velocities, which were observed at the periphery of the specimen. Lower velocities were observed in the central area of the specimen, which corresponded to the location of the pith in the specimen.

A number of graphs were generated from data of the stress-wave velocity measurements collected at the test points of the cross-sections of the specimens. Two graphs were generated for each specimen, one for Side A and another one for Side B. The graphs represent a number of lines connecting points of equal velocity, which were obtained by interpolation between the values that were actually measured. Here, the term used to refer to such lines is ‘velocity isolines’, while ‘velocity isoline graphs’ is the term used to describe the generated graphs. Figure 5 shows the graph for Side A of Specimen 3 and a picture of the cross-section tested. In the graph, the area with the lowest values corresponds to the area where the pith is located. Such a relationship was repeated for all the cross-sections tested.

A statistical analysis was performed to assess the effect of distance to pith on wave propagation velocity. A total of 425 observations were analysed and classified. The extreme values were excluded from the analysis, and distance was considered as the independent variable or factor. The level of the variable was the same for all the observations: one centimetre of distance to pith. Thus, 12 groups were defined, as shown in Figure 6. A number was assigned to each group

Editorial Office, TU MÃ¼nchen, Holzforschung MÃ¼nchen, Winzererstr. 45, 80797 MÃ¼nchen, Germany

according to the distance classification shown in Figure 6. Table 1 summarizes the descriptive statistics for these groups.

A Kolmogorov-Smirnov test was performed for all the observations. At 0.05 significance level, velocity was normally distributed. The average value was 1797.052 ± 318.324 m/s. At 95% confidence interval, the lower limit was 1766.701 m/s and the upper limit was 1827.402 m/s.

A Levene test for equality of variances was used to test the null hypothesis that the population variances were equal. Equality of variances was accepted for a test statistic of 1.617, with 11 and 413 degrees of freedom, and 0.091 significance for a level of 1 or 5.

Following the tests for normality and equality of variances, it was determined whether the velocity of stress-wave propagation measured on the cross-sections of the specimens was influenced by the distance from test point to pith. For that purpose, it was studied whether the average velocity varied depending on the distance group considered. A one-factor ANOVA was carried out with velocity as the dependent variable and distance to pith as the factor, and the null hypothesis that the means of the distance groups were equal was tested. Table 2 shows the results obtained from the analysis. Given that significance $p = 0$ at any significance level, the null hypothesis that the means were equal was rejected.

To determine which groups had different means, a post-hoc multiple comparison was performed. The Tukey honestly significant difference procedure was used to test the difference between each pair of means at 0.05 significance level. Table 3 summarizes the results of the comparison between the means of the measurements for Group 1 (0.0 mm < distance to pith ≤ 10.0 mm) and for the rest of the groups.

The mean for Group 1 showed significant differences when compared to the means for Groups 5 to 12 (distance to pith larger than 40.0 mm). Therefore, significant differences were found between tests performed near the pith (Groups 1 and 4) and tests performed farther from the pith (Groups 5 to 12).

Linear regression analysis between distance to pith and longitudinal stress-wave velocity was performed. Distance to pith was the independent variable and longitudinal stress-wave velocity was the dependent variable. Overall, 12 intervals of 10 mm were considered, coinciding with the groups shown in Figure 6. A velocity value was assigned to each 10-mm interval or distance group that corresponded to the mean value of the velocities measured for the corresponding interval. Two analyses were performed per specimen, one for each of the sides tested.

Pearson's correlation coefficient was determined to check whether there was linear correlation between the variables. Table 4 shows the results obtained for the different specimens. According to the results, distance to pith and mean velocity were positively or directly correlated at 0.05 significance level. ANOVA was conducted to check whether the regression fit could be considered statistically appropriate; Table 4 shows the results obtained from the analysis. Again, all the regressions were statistically appropriate at 0.05 significance level.

Figure 7 shows the values of the variables and the regression line obtained, and includes the regression equation and the value of the coefficient of determination R^2. The results of the coefficient of determination (R^2) suggest that the regression line accounts for over 90% of the variance in mean longitudinal stress-wave velocity for Specimen 1, Side A; Specimen 4, Side B and Specimen 6, Side A. The regression line accounts for over 80% of the variance for Specimen 1, Side B;

Specimen 2 (both sides) and Specimen 3 (both sides). For Specimen 4, Side A and Specimen 5 (both sides), the regression line accounts for over 70% of variance in mean longitudinal stress-wave velocity. The fit of the regression model was poorer for Specimen 6, Side B.

Considering variation in velocity at 10-mm intervals, the mean value of the increase in velocity at each 10-mm interval was 68.2895 m/s, at 95% confidence interval, with a lower limit of 43.0104 and an upper limit of 93.5688 m/s.

Figure 8 shows the results of linear regression analysis between mean longitudinal stress-wave velocity and distance to pith considering all the tests performed. The fit of the regression line to the values of mean velocity was $R^2 = 0.96$, which suggests that variation in velocity was caused by distance to pith. In addition, Figure 8 shows an increase in mean velocity with the increase in distance to pith, which reveals the velocity gradient in the wood from bark to pith. Considering the fit obtained, the velocity gradient was 67.642 m/s (0.13 coefficient of variation) at every 10-mm increase in distance from test position to pith.

Conclusion

The results obtained for longitudinal stress-wave velocity were in the range of 1167 to 2821 m/s. The groups used to classify distance to pith, divided into10-mm intervals, showed to be suitable for the analysis of variation in velocity.

ANOVA results for the relationship between distance to pith and mean velocity for each group revealed that the mean velocity values measured near the pith

Editorial Office, TU MÃ¼nchen, Holzforschung MÃ¼nchen, Winzererstr. 45, 80797 MÃ¼nchen, Germany

(between 0.0 and 40.0 mm) were significantly different from measurements collected at larger distances.

Positive correlations were found between distance to pith and mean velocity for the analysed measurements. The linear regression analyses performed on the results obtained for each specimen showed correlation coefficients above 0.80 in most cases.

An overall coefficient of determination R^2= 0.96 was obtained from the regression analysis of mean velocity according to the different distance intervals considered. The fitted line showed an increase in longitudinal stress-wave velocity with the increase in distance to pith. Such an increase amounted to 67.642 m/s every10-mm increase in the distance from test point to pith.

The next phase of our research will focus on determining the influence of specimen length on the accuracy of fit for the analyzed parameters.

Acknowledgements

This research has been co-funded by the Spanish Ministry of Science and Technology within the framework of Research Project BIA 2004-07146 'Validation of Resistograph as a Tool for the Assessment and Characterization of Structural Timber' and by the Galician Government *Xunta de Galicia, Consellería de Innovación e Industria* within the framework of the project PGIDIT05PXIC29102PN.

Integrity of research and reporting

The authors declare that they have no conflict of interest.

Editorial Office, TU MÃ¼nchen, Holzforschung MÃ¼nchen, Winzererstr. 45, 80797 MÃ¼nchen, Germany

References

Adamopoulos S, Passialis C, Voulgaridis, E (2007) Strength properties of juvenile and mature wood in black locust (Robinia pseudoacacia L.). Wood Fiber Sci. 39:241-249.
Brashaw BK, Wang XP, Ross RJ, Pellerin RF (2004) Relationship between stress wave velocities of green and dry veneer. For. Prod. J. 54:85-89.
Chauhan SS, Entwistle KM, Walker JCF (2007) Search for a relationship between stress wave velocity and internal stresses in eucalypts and radiata pine. Holzforschung 61:60-64.
Chauhan SS, Walker JCF (2006) Variations in acoustic velocity and density with age, and their interrelationships in radiata pine. For. Ecol. Man. 229:388-394.
Chauhan SS, Entwistle KM, Walker JCF (2005) Differences in acoustic velocity by resonance and transit-time methods in an anisotropic laminated wood medium. Holzforschung 59:428-434.
Deflorio G, Fink S, Schwarze FWMR (2008) Detection of incipient decay in tree stems with sonic tomography after wounding and fungal inoculation. Wood Sci. Technol. 42:117-132
Divos F, Denes L, Íñiguez G (2005) Effect of cross-sectional change of a board specimen on stress wave velocity determination. Holzforschung 59:230-231.
Divos F, Szalai L (2003) Tree evaluation by acoustic tomography. In: Proceedings of the 13th International Symposium on Nondestructive Testing of Wood. pp. 251-256.
Grabianowski M, Manley B, Walker JCF (2006) Acoustic measurements on standing trees, logs and green lumber. Wood Sci. Technol. 40:205-216.
Han GP, Wu QL, Wang XP (2006) Stress-wave velocity of wood-based panels: Effect of moisture, product type, and material direction. For. Prod. J. 56:28-33.
Íñiguez G, Arriaga F, Esteban M, Argüelles R (2007) Vibration methods as non-destructive tool for structural properties assessment of sawn timber. Informes de la Construcción 59:97-105.
Katz JL, Spencer P, Wang Y, Misra A, Marangos O, Friis L (2008) On the anisotropic elastic properties of woods. J. Mat. Sci. 43:139-145.
Lawday G, Hodges PA (2000) The analytical use of stress waves for the detection of decay in standing trees. Forestry 73:447-456.
Lee JJ, Oh JK (1999) Stress-wave technique for detecting decay in ancient structures. In: Proceedings of the Eleventh International Symposium on Nondestructive Testing of Wood. pp. 161-167.
Marchal M, Jacques D (1999) Evaluation of two acoustic methods of MOE determination for young hybrid larch wood (Larix x eurolepis Henry). Comparison with a standard method by static bending. Ann. For. Sci. 56:333-343.
Nanami N, Nakamura N, Arima T, Okuma M (1992) Measuring the properties of standing tress with stress waves. 1. The method of measurement and the propagation path of the waves. Mokuzai Gakkaishi 38:739-746.
Rinn F (1999) Device for investigating materials. International Application No.: PCT/DE2000/001467
Rinn F (2003) Technische Grundlagen der Impuls-Tomographie. Baumzeitung 8:29-31.
Rinn F (2004) Statische Hinweise im Schall-Tomogramm von Bäumen. Stadt und Grün 7:41-45.
Rinntech (2005) Artotom® 3-D Tree Impulse Tomograph. User Manual. Copyright © Frank Rinn, Heidelberg.
Rippy RC, Wagner FG, Gorman TM, Layton HD, Bodenheimer T (2000) Stress-wave analysis of Douglas-fir logs for veneer properties. For. Prod. J. 50:49-52.
Ross RJ, Ward JC, Tenwolde A (1994) Stress wave nondestructive evaluation of wetwood. For. Prod. J. 44:79-83.
Ross RJ, Zerbe JI, Wang XP, Green DW, Pellerin RF (2005) Stress wave nondestructive evaluation of Douglas-fir peeler cores. For. Prod. J. 55:90-94.
Ross RJ, Willits SW, von Segen W, Balck T, Brashaw BK, Pellerin RF (1999) A stress-wave-based approach to nondestructive evaluation of logs for assessing potential veneer quality using small-diameter ponderosa pine. In: Proceedings of the Eleventh International Symposium on Nondestructive Testing of Wood. pp. 123-126.
Simpson WT, Wang XP (2001) Relationship between longitudinal stress wave transit time and moisture content of lumber during kiln-drying. For. Prod. J. 51:51-54.
Wagner FG, Gorman TM, Wu SY (2003) Assessment of intensive stress-wave scanning of Douglas-fir trees for predicting lumber MOE. For. Prod. J. 53:36-39.
Wang SY, Lin CJ, Chiu CM (2005) Evaluation of wood quality of Taiwanian trees grown with different thinning and pruning treatments using ultrasonic-wave testing. Wood Fiber Sci. 37:192-200.

Editorial Office, TU MÃ¼nchen, Holzforschung MÃ¼nchen, Winzererstr. 45, 80797 MÃ¼nchen, Germany

Wang X, Divos F, Pilon C, Brashaw BK, Ross RJ, Pellerin RF (2004a) Assessment of decay in standing timber using stress wave timing nondestructive evaluation tools. General Technical Report FPL-GTR-147. USDA Forest Service, Forest Products Laboratory, 12 pp.
Wang XP, Ross RJ, Green DW, Brashaw B, Englund K, Wolcott M (2004b) Stress wave sorting of red maple logs for structural quality. Wood Sci. Technol. 37:531-537.
Wang, XP, Ross RJ, Brashaw BK, Punches J, Erickson JR, Forsman JW, Pellerin RF (2004c) Diameter effect on stress-wave evaluation of modulus of elasticity of logs. Wood Fiber Sci. 36:368-377.
Wang XP, Ross RJ, Mattson JA, Erickson JR, Forsman JW, Geske EA, Wehr MA (2002) Nondestructive evaluation techniques for assessing modulus of elasticity and stiffness of small-diameter logs. For. Prod. J. 52:79-85.
Wang J, Biernacki JM, Lam F (2001a) Nondestructive evaluation of veneer quality using acoustic wave measurements. Wood Sci. Technol. 34:505-516.
Wang XP, Ross RJ, McClellan M, Barbour RJ, Erickson JR, Forsman JW, McGinnis GD (2001b) Nondestructive evaluation of standing trees with a stress wave method. Wood Fiber Sci. 33:522-533.
Wu QL (1999) Influence of moisture on stress-wave properties of wood-based panels. In: Proceedings of the Eleventh International Symposium on Nondestructive Testing of Wood. Madison, WI. September 9-11 1998 pp. 19-26.

Figure legends

Figure 1. Dimensions of specimens (1) and cross-sections tested (2)
Abb. 1 Prüfkörperabmessungen (1) und Messstellen (2)

Figure 2. Distribution of sensor positions for performing the tests parallel to the grain

Abb. 2 Verteilung der Messstellen für die Durchführung der Messungen in longitudinaler Richtung

Figure 3. Equipment prepared to perform a test on the cross-sections, with sensors located aligned at opposite positions on both sides
Abb. 3 Versuchsvorrichtung mit den Sensoren an den jeweils entsprechenden Stellen an beiden Hirnholzenden

Figure 4. Example of acoustic tomogram, obtained for specimen 2 using 10 sensors

Abb. 4 Beispiel eines akustischen Tomogramms des Prüfkörpers 2 unter Verwendung von 10 Sensoren

Figure 5. Velocity (x 100 m/s) isoline graph obtained by interpolation of the velocities measured at every test location for specimen 3, side A.
Abb. 5 Isolinien der Geschwindigkeit (x 100 m/s) auf Seite A von Prüfkörper 3; bestimmt durch Interpolation der an jeder Messstelle ermittelten Geschwindigkeiten

Figure 6. Test groups established according to distance to pith (the picture corresponds to specimen 4)
Abb. 6 Versuchsgruppen unterteilt nach der Entfernung zur Markröhre (Bild entspricht Prüfkörper 4)

Figure 7. Linear regression analysis of mean stress-wave propagation velocity at 10-mm intervals, according to specimen and side tested

Abb. 7 Lineare Regressionsanalyse der mittleren Stosswellengeschwindigkeit in Abhängigkeit der Markabstände (in Intervallen von 10 mm) an beiden Hirnholzenden aller Prüfkörper

Figure 8. Linear regression analysis of mean stress-wave propagation velocity at 10-mm intervals for distances to pith in the range 10.00 to 120.0 mm for all tests performed

Abb. 8 Lineare Regressionsanalyse der mittleren Stosswellengeschwindigkeit in Abhängigkeit der Markabstände im Bereich 10 bis 120 mm (in Intervallen von 10 mm) für alle durchgeführten Versuche

Editorial Office, TU MÃ¼nchen, Holzforschung MÃ¼nchen, Winzererstr. 45, 80797 MÃ¼nchen, Germany

Table 1 Descriptive statistics for the groups of observations
Tabelle 1 Statistische Werte der Versuchsgruppen

Group	d (mm)	N	$\overline{X}$	SD	CV
1	$0 < d \leq 10.0$	11	1475	171	0.12
2	$10.0 < d \leq 20.0$	26	1477	212	0.14
3	$20.0 < d \leq 30.0$	36	1594	203	0.13
4	$30.0 < d \leq 40.0$	47	1599	228	0.14
5	$40.0 < d \leq 50.0$	48	1778	281	0.16
6	$50.0 < d \leq 60.0$	61	1774	286	0.16
7	$60.0 < d \leq 70.0$	60	1871	268	0.14
8	$70.0 < d \leq 80.0$	52	1939	305	0.16
9	$80.0 < d \leq 90.0$	32	1973	289	0.15
10	$90.0 < d \leq 100.0$	36	1990	283	0.14
11	$100.0 < d \leq 110.0$	11	2223	292	0.13
12	$110.0 < d \leq 120.0$	5	2148	314	0.15

Key:
d: Distance to pith (mm)
N: Number of observations per group
$\overline{X}$: Mean value of longitudinal stress-wave velocity per group (m/s)
SD: Standard deviation
CV: Coefficient of variation

Table 2 ANOVA for velocity observations classified into groups according to distance from test location to pith
Tabelle 2 ANOVA für die Geschwindigkeit in Abhängigkeit der Versuchsgruppen

Source of variation	Sum of squares	df	Mean Square	F	Sig.
Between groups	13505151	11	1227741	17	0.000
Within groups	29458830	413	71329		
Total	42963981	424			

Editorial Office, TU MÃ¼nchen, Holzforschung MÃ¼nchen, Winzererstr. 45, 80797 MÃ¼nchen, Germany

Table 3 Results of Tukey HSD test for the comparison between the measurements for distance group 1 and the rest of groups

Ergebnisse der Tukey HSD Tests. Vergleich der Messwerte der Gruppe 1 mit den jeweils anderen Gruppen

Test	(I) Distance to pith	(J) Distance to pith	Difference of means (I-J)	Standard error	Sig.	95% Confidence interval Upper limit	95% Confidence interval Lower limit
Tukey HSD test	Group 1	Group 2	-2	96	1.000	-317	314
		Group 3	-119	92	0.980	-422	183
		Group 4	-124	89	0.965	-418	170
		Group 5	-304(*)	89	0.035	-597	-10
		Group 6	-299(*)	87	0.034	-586	-11
		Group 7	-396(*)	88	0.000	-684	-108
		Group 8	-464(*)	89	0.000	-756	-173
		Group 9	-498(*)	93	0.000	-805	-192
		Group 10	-515(*)	92	0.000	-817	-212
		Group 11	-748(*)	114	0.000	-1123	-374
		Group 12	-673(*)	144	0.000	-1147	-200

(*) The difference of means is significant at 0.05 significance level

Table 4 Results of linear regression analysis between variables and of ANOVA for regression

Tabelle 4 Korrelationskoeffizient und ANOVA Ergebnisse bei linearer Regression

Identification of results	Pearson correlation		ANOVA for regression			
	Coefficient	Sig.*	df[1]	df[2]	F	Sig.
Specimen 1-Side A	0.95	0.000	1	12	106	0.000
Specimen 1-Side B	0.97	0.000	1	11	149	0.000
Specimen 2-Side A	0.90	0.000	1	8	35	0.000
Specimen 2-Side B	0.95	0.000	1	11	107	0.000
Specimen 3-Side A	0.92	0.000	1	8	41	0.000
Specimen 3-Side B	0.91	0.000	1	9	43	0.000
Specimen 4-Side A	0.85	0.000	1	9	24	0.001
Specimen 4-Side B	0.97	0.000	1	8	117	0.000
Specimen 5-Side A	0.84	0.005	1	7	17	0.005
Specimen 5-Side B	0.88	0.002	1	7	24	0.002
Specimen 6-Side A	0.97	0.000	1	7	128	0.000
Specimen 6-Side B	0.72	0.029	1	7	8	0.029

*: One-sided significance

1: Degrees of freedom for the regression sum of squares

2: Degrees of freedom for the residual sum of squares

Editorial Office, TU MÃ¼nchen, Holzforschung MÃ¼nchen, Winzererstr. 45, 80797 MÃ¼nchen, Germany

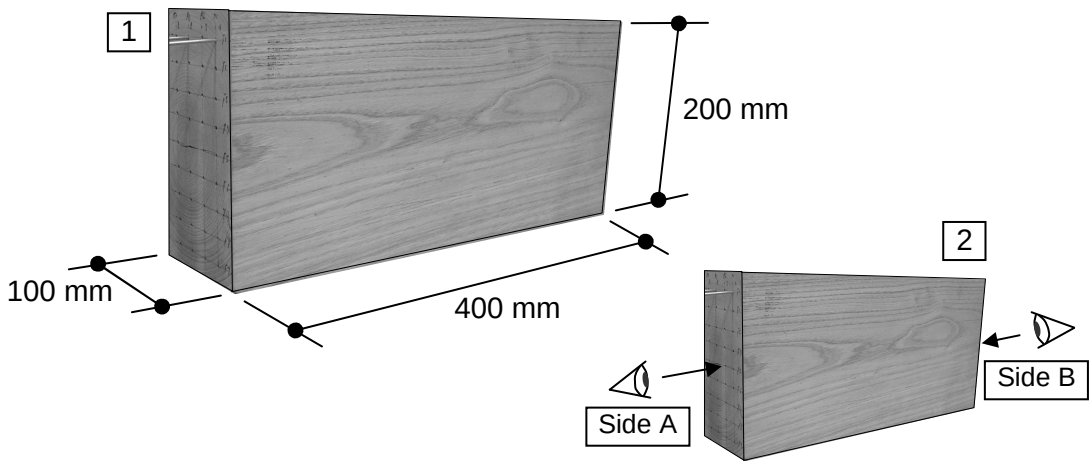

Fig.1

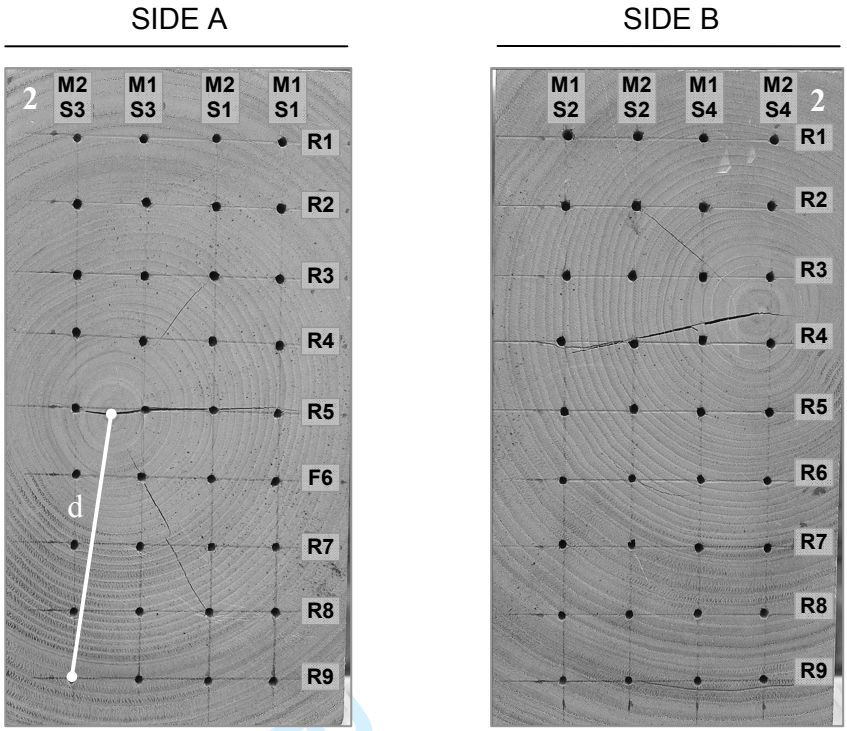

Key:
2: Specimen number.
S1: Sensor No. 1.
S2: Sensor No. 2.
S3: Sensor No. 3.
S4: Sensor No. 4.
Ri: Row number.

M1: Column of measurements No. 1. First position of receiver
M2: Column of measurements No. 2. Second position of receiver
d: Example of distance to pith measured at every location

Fig.2

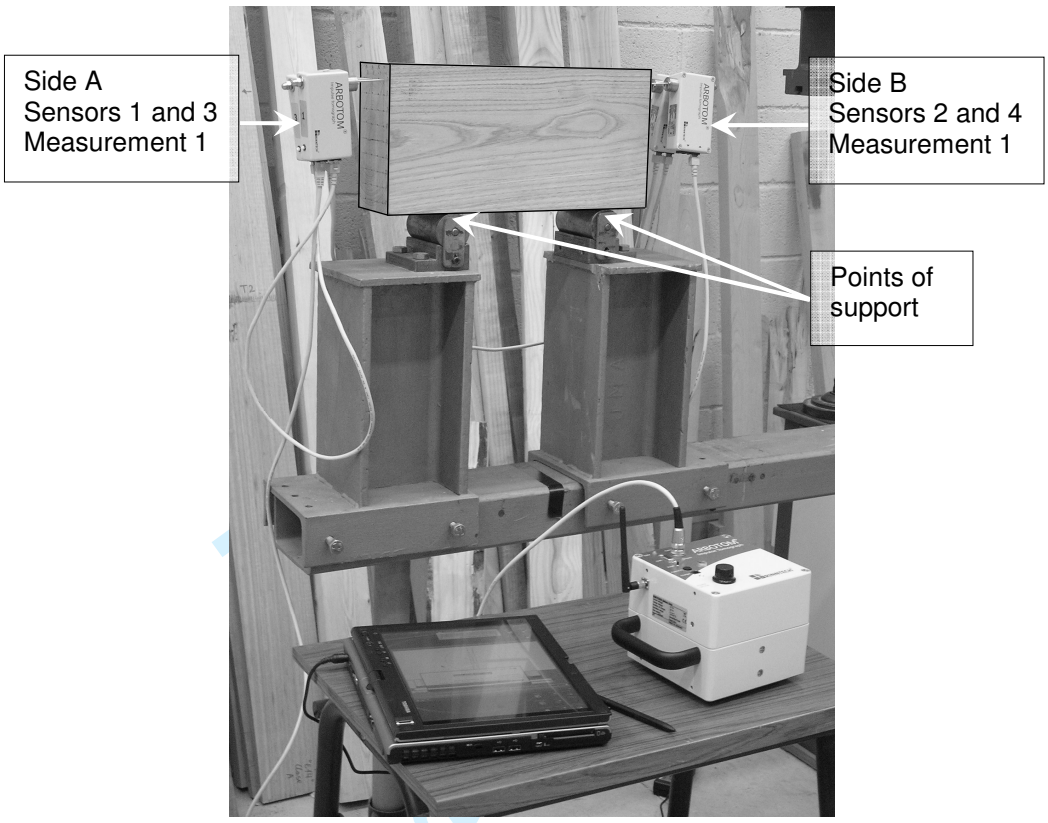

Fig.3

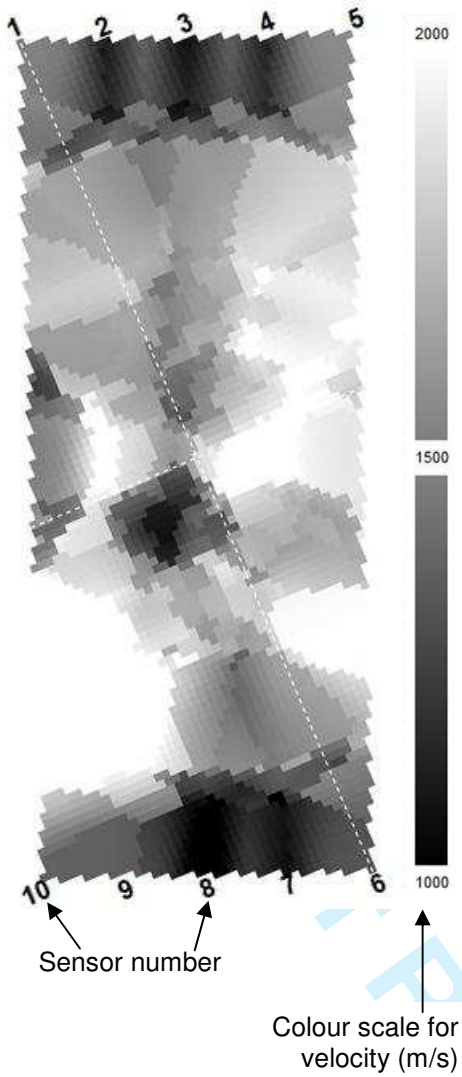

Fig.4

Editorial Office, TU MÃ¼nchen, Holzforschung MÃ¼nchen, Winzererstr. 45, 80797 MÃ¼nchen, Germany

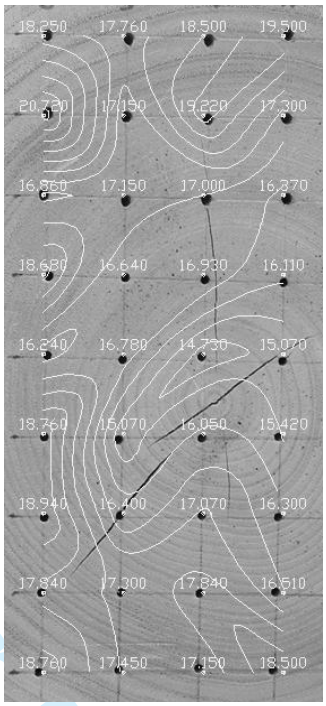

Fig.5

Editorial Office, TU MÃ¼nchen, Holzforschung MÃ¼nchen, Winzererstr. 45, 80797 MÃ¼nchen, Germany

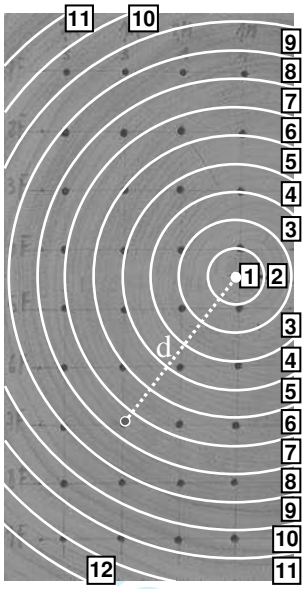

G	d (mm)
1	0.0 < d ≤ 10.0
2	10.0 < d ≤ 20.0
3	20.0 < d ≤ 30.0
4	30.0 < d ≤ 40.0
5	40.0 < d ≤ 50.0
6	50.0 < d ≤ 60.0
7	60.0 < d ≤ 70.0
8	70.0 < d ≤ 80.0
9	80.0 < d ≤ 90.0
10	90.0 < d ≤ 100.0
11	100.0 < d ≤ 110.0

Key:
G: Test groups according to distance
d: Distance from test location to pith

Fig.6

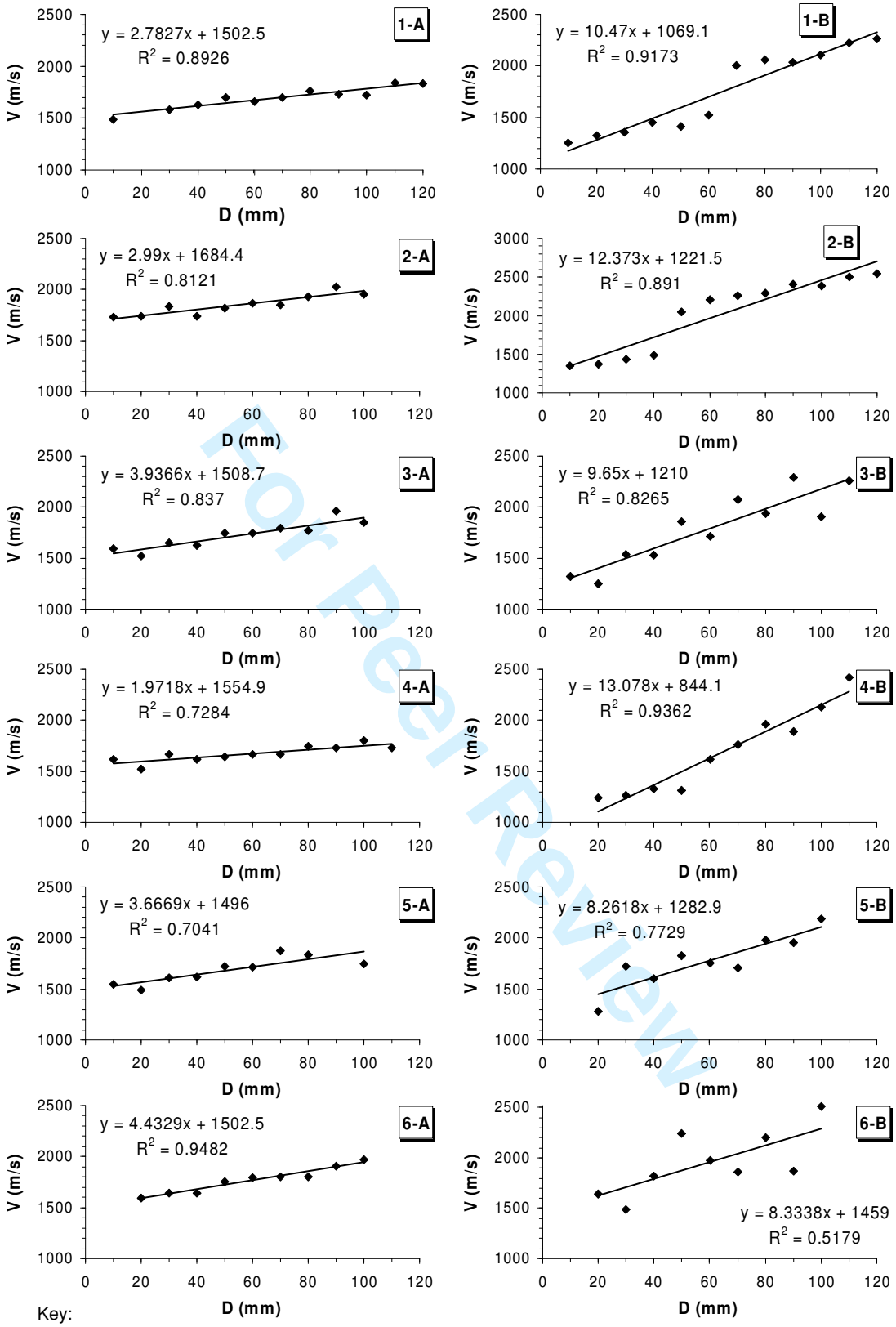

Key:
D: Distance to pith at 10-mm intervals
V: Mean velocity of the observations at each interval

1-A: Specimen number-Side tested

Fig.7

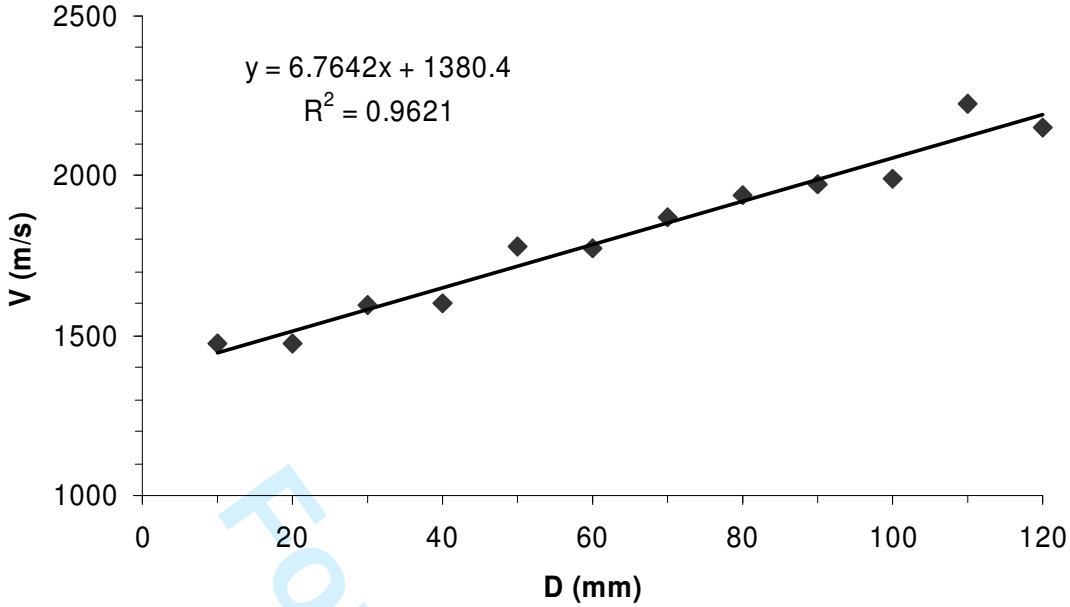

Fig.8

Editorial Office, TU MÃ¼nchen, Holzforschung MÃ¼nchen, Winzererstr. 45, 80797 MÃ¼nchen, Germany